ELE438—Lab Report

RN: 200327363

December 2025

Contents

1 Modelling

1.1 First Order Input Response

The original LTI model of the helicopter assumes control of the elevation and pitch rates ($\dot{E}(t)$ and $\dot{\Psi}(t)$) as if the steady-state fan force is applied instantaneously; this is not the case in the real system as the fans have a finite response time.

1.1.1 Model Derivation

New states $V_a(t)$ and $V_b(t)$ were added to represent the *actual inputs*, each modelled as a first order response with unit gain and time constant τ_F equal to that of the fans' first order approximation, $\tau_F = 0.87\,\text{s}$. This was determined with system identification on the dynamic response load cell data. In the combined model, the new states substitute for the terms involving $U_{a,b}(t)$, and control inputs are applied exclusively to them rather than on the pitch and elevation rates. This yields the combined LTI model ($x = x(t),\ u = u(t),\ y = y(t)$ for compactness)

$$\dot{\bar{x}} = \bar{A}\bar{x} + \bar{B}u, \qquad y = C\bar{x} + Du$$

where the modified elements denoted by $\bar{\cdot}$ are

$$\bar{x} = \begin{bmatrix} E & \Psi & \Theta & \dot{E} & \dot{\Psi} & \dot{\Theta} & V_a & V_b \end{bmatrix}^T,$$

$$\bar{A} = \begin{bmatrix} 0 & 0 & 0 & 1 & 0 & 0 & 0 & 0 \\ 0 & 0 & 0 & 0 & 1 & 0 & 0 & 0 \\ 0 & 0 & 0 & 0 & 0 & 1 & 0 & 0 \\ -\frac{k_E}{J_E} & 0 & 0 & -\frac{c_E}{J_E} & 0 & 0 & \frac{l_1\,\alpha\,k_a}{J_E} & \frac{l_1\,\alpha\,k_a}{J_E} \\ 0 & -\frac{k_\Psi}{J_\Psi} & 0 & 0 & -\frac{c_\Psi}{J_\Psi} & 0 & \frac{l_2\,\alpha\,k_a}{J_\Psi} & -\frac{l_2\,\alpha\,k_a}{J_\Psi} \\ 0 & \frac{-2l_1\,(\alpha\,k_a V_e + \beta)}{J_\Theta} & 0 & 0 & 0 & -\frac{c_\Theta}{J_\Theta} & 0 & 0 \\ 0 & 0 & 0 & 0 & 0 & 0 & -\frac{1}{\tau_F} & 0 \\ 0 & 0 & 0 & 0 & 0 & 0 & 0 & -\frac{1}{\tau_F} \end{bmatrix}, \qquad \bar{B} = \begin{bmatrix} 0 & 0 \\ 0 & 0 \\ 0 & 0 \\ 0 & 0 \\ 0 & 0 \\ 0 & 0 \\ \frac{1}{\tau_F} & 0 \\ 0 & \frac{1}{\tau_F} \end{bmatrix}$$

With $V_e = U_e$. Note that spring and damping effects have been added to the elevation axis, as well as damping to the travel axis, following this the notation for the spring coefficients is k_x, and damping c_x.

An equivalent method for this modification is to make the additional states the fan forces $F_{a,b}$, rather than delayed inputs, this was experimented with. In that case, the original model in Mini Assignment 1—before the $(\alpha\,k_a\,U_{a,b} + \beta)$ substitution—is used, and the fan model is taken directly from the system identification step. The reason that the current method was opted for is to improve the approximation of the linear steady-state response, allowing for a nonzero y-intercept, and to take the average across the fans' range, rather than from a single measurement of the dynamic response. In the case of the direct system identification model, the steady-state response is only parameterised by the gain, missing out on the flexibility afforded by the β term.

1.1.2 Experiment on the Real System

To demonstrate the improvement in comparison to the original model, an experiment was designed using the real helicopter pitch axis. As opposed to an experiment involving the other axes, the pitch axis alone is ideal because:

- The modelled pitch axis dynamics do not depend on the other axes
- The modelled dynamics are linear (unlike the other two)

- Model mismatch is reduced because there are less moving parts
- It can be easily isolated by holding the other two axes still.

If the model is improved, the simulated response should match the real response more closely than the original model.

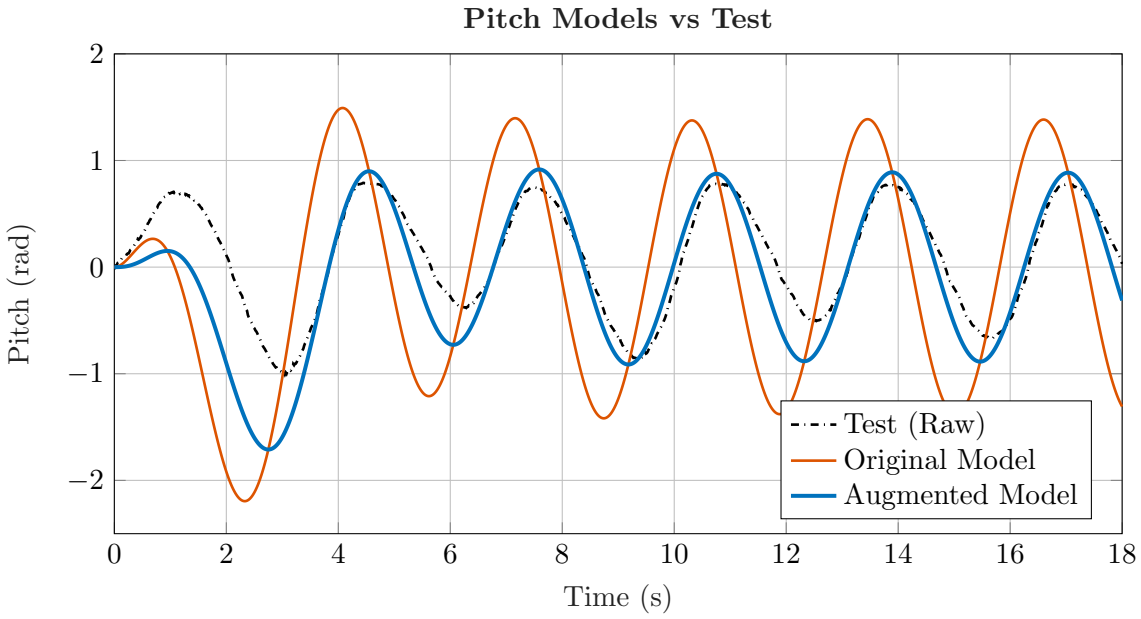

Figure 1: *Pitch axis experimental data with augmented model vs old model*

During the experiment, sine and cosine inputs were applied to the fans (out of phase with each other) to oscillate the pitch axis. The amplitude of the input signals were in the range $[0.3,\ 10]$ to eliminate the nonlinear fan behaviour below the voltage threshold, the frequency of the signals is 2 rad/s—this was determined manually to get a response that spanned a large portion of the pitch axis. Using the same series of inputs, the response from each linear model was simulated. Figure 1 illustrates the simulated responses in comparison to the test data. The MSE of the original model response was 0.8358, and the MSE of the new model was 0.0945—this shows a marked improvement. Since the other axes are functions of the pitch axis, it is a reasonable conclusion that the accuracy of the model is improved overall.

1.2 Minor Model Improvements

In the original material, the inertia of the travel axis, J_Θ, was assumed equal to the inertia of the elevation axis, $J_E = 2m_1l_1^2 + m_2l_3^2$. The equation of the inertia given a set of point-masses, m_i and their distances to the axis, l_i, is $\sum m_i l_i^2$. At the level hover condition, looking along the travel axis, the distance from a fan with mass m_1, is $l_F = \sqrt{l_1^2 + l_2^2}$. This resolves to $J_\Theta = 2m_1(l_1^2 + l_2^2) + m_2l_3^2$, which has an extra term in l_2.

As briefly mentioned prior, spring and damping effects were added to the elevation and travel axes. To converge on a set of spring and damping coefficients for all axes, a test input/output log (during normal controlled operation) was used to compare against a script simulation using the logged inputs, with these parameters adjusted by hand to fit. System identification techniques were experimented with to identify these parameters, but the hand-adjustment gave better results. The simulation implemented nonlinear dynamics through a MATLAB function handle and 4th-order Runge-Kutta integration.

2 Control Design

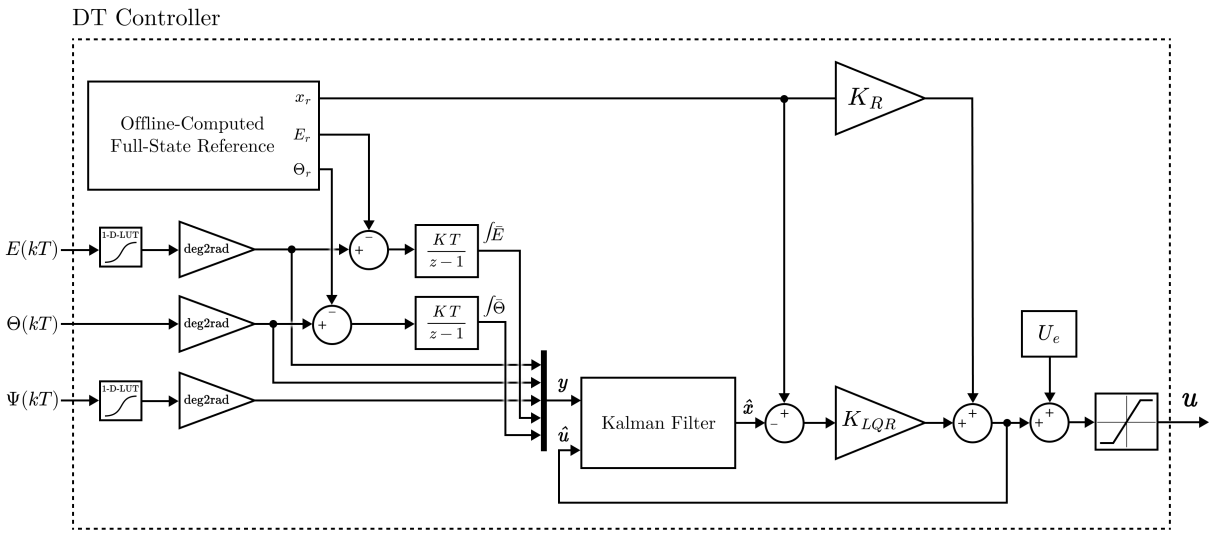

Figure 2: *Controller block diagram*

Figure 2 shows the controller block diagram in the dashed box.

2.1 Integral Action Model

The state-space model was augmented by two integral states, $x_i = \begin{bmatrix} \int E & \int \Theta \end{bmatrix}^T$. Since integral action is required for zero-offset tracking, these are required to meet the specification. It was found that integral action for the pitch axis was not necessary, as it settles to equilibrium with a zero input. The integral states are with reference to a setpoint, so the references for the corresponding position states are subtracted before integration through the discrete-time integrator blocks. This was done explicitly in the Simulink model, as adding them to C was required for system observability. Rather than splitting into separate integral action and state feedback gains, a single state-space system and feedback gain was chosen for convenience with trying other control architectures and script simulations.

2.2 Kalman Filter Tuning

To characterise the noise from the measurements in C, a sample of data was taken of the helicopter at rest, unforced. After removing bias, the MATLAB `cov` function was used to automatically calculate R in the Kalman Filter. To characterise the process noise, a test log was used to compare against a linear simulation with the same input series—taking the covariance of the differences. This was more difficult as the test logs need to be smooth and accurate, a median filter and a moving mean filter (offset for the induced lag) were used in conjunction. Though these tests gave a starting point, Q was further adjusted by hand with tests.

2.3 Reference Generation

Two reference generators were made: a finite impulse response (FIR) filter method and a nonlinear optimisation method. These can be selected through Simulink Variants.

2.3.1 FIR Method

A second-order FIR filter was developed for the Θ and $\dot{\Theta}$ reference as the feasible option for real-time computation on an embedded system. Using the Lecture 10 notes as a reference, the

travel axis reference is user-parameterised by the transition time T_{trans} and maximum desired pitch angle $\Psi_{\max}$. The method in the notes uses $A_{\max}$, which can be made a function of Ψ to be more intuitive. The maximum travel axis angular acceleration that can be achieved for a given pitch angle is limited by the maximum force of the fans, $2F_{\max}$, at the distance l_F (derived earlier), and the inertia about the axis, J_Θ.

$$\alpha_{\max}(\Psi) = \frac{2F_{\max}\,\sin(\Psi)\,l_F}{J_\Theta}$$

Given a velocity calculated from transition displacement (180°) and time, $v_{\text{trans}} = s_{\text{trans}}/T_{\text{trans}}$, a smoothing kernel of time-width $T_{\text{kern}} = v_{\text{trans}}/\alpha_{\max}$ is twice convolved with the rectangular velocity profile. The position trajectory is the integral of this velocity profile.

The FIR reference makes the assumption that the maximum pitch angle and maximum fan force can be achieved instantly; therefore, it is not precisely feasible, but it is a smooth reference and can be computed very quickly.

2.3.2 Nonlinear Optimisation Method

Using the nonlinear dynamic model derived from the Euler-Lagrange modelling and a first-order approximation of the fan response, full-state optimal transition trajectories were computed with a nonlinear program (NLP) using direct collocation in ICLOCS2. The continuous-time optimisation problem was formulated as

$$\begin{aligned}
\min_{U_a,\,U_b} \quad & \int_0^{t_f} U_a(t)^2 + U_b(t)^2\,dt \\
\text{s.t.} \quad & \dot{x}(t) = f(t,\,x(t),\,u(t)) \\
& -10^\circ \le E(t) \le 10^\circ, \quad -20^\circ \le \Theta(t) \le 200^\circ \\
& E(0) = E(t_f) = \Theta(0) = 0^\circ, \quad \Theta(t_f) = 180^\circ
\end{aligned}$$

The final time t_f is left free as it was found that the solution transitions within a good margin of the specification. The above formulation is for the outward trajectory; for the return, the boundary constraints on Θ are reversed.

The result is a robust and dynamically feasible reference with no input saturation, however, implementing nonlinear optimisation in a real-time embedded system is dubious, as the NLP is slow and is not guaranteed to converge to a solution. Since the embedded implementation is not given as a priority, this method will be used for the results to maximise the performance.

2.4 Feedback and Feedforward Gains

Using the model with augmented integral states, an LQR feedback gain, K_{LQR}, was designed. The model simulation was tuned such that the trajectory for the same controller matched the test reasonably. Cost tuning could be performed more quickly with the simulated model; once a good level of control was achieved, the costs were fine-tuned to the physical model. Using the optimised trajectory, it was found that R could be set very low as the reference is already optimised for minimum effort, allowing it to track closely throughout the transition. Minimal cost in Q was set on the pitch axis, using only the pitch rate cost and reference to get the system moving at the beginning of the transition. High cost is set on the travel rate to achieve minimal overshoot and oscillation. As minimal oscillation and overshoot was experienced on the elevation axis, it was not costed highly overall—the integral action does most of the work to maintain tracking. The feedforward gain K_r was calculated using the standard formula.

3 Results

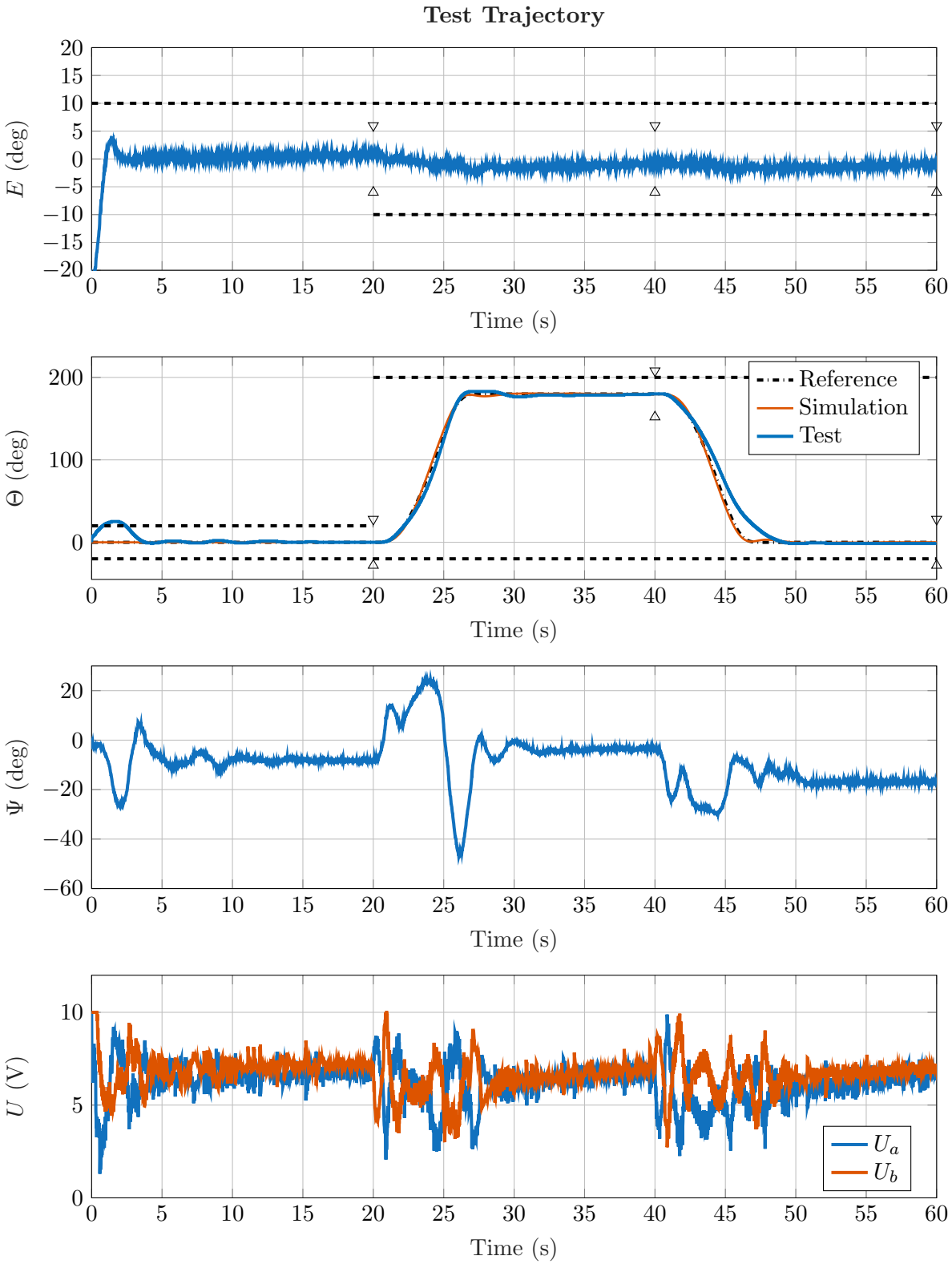

Figure 3: *Positions and inputs from a sample test*

3.1 Discussion

Figure 3 shows a sample of recorded positions and inputs from a test. In summary, all performance criteria were met apart from the violation of the travel bound at the beginning of the trajectory. The overshoot bounds are illustrated with dashed lines, and the transition points are indicated by the arrow markers whose gaps correspond to the settling specification at that time. Input saturation happens briefly at the beginning of the test and during the initiation of a transition. In the test shown in Figure 3, U_a is saturated for 0.025% of the trajectory, and U_b for 0.725%.

3.1.1 Travel Bound Violation

On every test, the system violated the travel bound of $+20°$, this seems almost independent of adjustments to the model values and controller tuning. Though the travel and pitch start at roughly zero, applying equal thrust to the fans (as shown at the very beginning of the input plot) causes the travel axis to move, and it settles to zero travel velocity with a nonzero pitch—this indicates an imbalance in the helicopter somewhere. Investigating the response when the pitch angle starts facing slightly the other way, it was observed that it still moves the travel axis in the opposite direction, which suggests that it is independent of the pitch angle. Similarly, the travel axis moves when the fans stop spinning, but not when dropped by hand.

A plausible explanation for this behaviour is to consider the inertia of the fan blades: as they spin up, conservation of angular momentum should cause the travel axis to rotate in the opposite direction. The rotational directions of the fans and the travel axis perturbation are opposite—consistent with this theory. Furthermore, the trajectory consistently lags behind the reference only on the return transition (which can be seen in Figure 3), where it is having to push against this torque; since this is not modelled in the simulation, it does not exhibit this behaviour, despite the rest of the trajectory being closely representative of the test.

Since the fans start at full thrust, inertia is quickly imparted into the axis; this can be partially resolved by detuning the elevation axis gains, but at the expense of tracking performance. A better option may be to have a smooth reference from the initial elevation to reduce the initial thrust to allow more time for the controller to compensate. The ideal solution (if this is the correct explanation) would be to use fans that spin in opposing directions.

This effect could be modelled and included in the state space system: the torque exerted by the fans on the travel axis is proportional to their angular accelerations and current draws. Therefore, this could be approximated onboard using a current sensor on the fans, or (less reliably) via state estimation. Since the fan force is proportional to the blade velocity (hence $V_{a,b}$), then the rate of change of the fan force is proportional to the blade acceleration. A second-order fan model is sufficient to model this effect, where $\dot{\Theta}$ is related to $\dot{V}_{a,b}$, which are estimated by the Kalman Filter; whole-system observability holds for this alteration and would require the addition of only two states.

3.1.2 Optimal Reference Generator

One of the key advantages of the full-state reference in comparison to the FIR method is the inclusion of the pitch and pitch rate references, as this is the principle axis of the fans. The pitch rate commands are very effective at initiating the transition; without them, the travel axis lags behind the reference, and overshoot increases. A model-based algorithm is required for a dynamically feasible full-state trajectory. However, the issue of an embedded implementation of the optimisation algorithm remains. Though it can be feasibly implemented on *an* embedded system, it certainly could not be implemented on the myDAQ with any reasonable performance. Either it could remain as an offline computation, or it could be approximated as a quadratic program, which can be implemented on embedded platforms at high speed—this would involve trading off some freedom in the problem formulation.